Published OnlineFirst May 16, 2012; DOI: 10.1158/0008-5472.CAN-12-0667

Cancer Research

miR-103/107 Promote Metastasis of Colorectal Cancer by Targeting the Metastasis Suppressors DAPK and KLF4

Hsin-Yi Chen, Yu-Min Lin, Hsiang-Ching Chung, et al.

Cancer Res 2012;72:3631-3641. Published OnlineFirst May 16, 2012.

Published OnlineFirst May 16, 2012; DOI: 10.1158/0008-5472.CAN-12-0667

miR-103/107 Promote Metastasis of Colorectal Cancer by Targeting the Metastasis Suppressors DAPK and KLF4

Hsin-Yi Chen[1], Yu-Min Lin[1,2], Hsiang-Ching Chung[1,2], Yaw-Dong Lang[1], Ching-Jung Lin[1,2], John Huang[3], Wei-Chi Wang[4], Feng-Mao Lin[4], Zhen Chen[5], Hsien-Da Huang[4], John Y.-J. Shyy[5], Jin-Tung Liang[3], and Ruey-Hwa Chen[1,2]

Abstract

Metastasis is the major cause of poor prognosis in colorectal cancer (CRC), and increasing evidence supports the contribution of miRNAs to cancer progression. Here, we found that high expression of miR-103 and miR-107 (miR-103/107) was associated with metastasis potential of CRC cell lines and poor prognosis in patients with CRC. We showed that miR-103/107 targeted the known metastasis suppressors death-associated protein kinase (DAPK) and Krüppel-like factor 4 (KLF4) in CRC cells, resulting in increased cell motility and cell–matrix adhesion and decreased cell–cell adhesion and epithelial marker expression. miR-103/107 expression was increased in the presence of hypoxia, thereby potentiating DAPK and KLF4 downregulation and hypoxia-induced motility and invasiveness. In mouse models of CRC, miR-103/107 overexpression potentiated local invasion and liver metastasis effects, which were suppressed by reexpression of DAPK or KLF4. miR-103/107–mediated downregulation of DAPK and KLF4 also enabled the colonization of CRC cells at a metastatic site. Clinically, the signature of a miR-103/107 high, DAPK low, and KLF4 low expression profile correlated with the extent of lymph node and distant metastasis in patients with CRC and served as a prognostic marker for metastasis recurrence and poor survival. Our findings therefore indicate that miR-103/107–mediated repression of DAPK and KLF4 promotes metastasis in CRC, and this regulatory circuit may contribute in part to hypoxia-stimulated tumor metastasis. Strategies that disrupt this regulation might be developed to block CRC metastasis. *Cancer Res; 72(14); 3631–41. ©2012 AACR.*

Introduction

Metastasis is responsible for most cancer mortality. The secondary growths arise through a multistep process, including invasion of tumor cells into the adjacent tissues, intravasation into the systematic circulation, survival in the circulation, extravasation from blood vessels, initiation and maintenance of micrometastases at distant sites, and ultimately the outgrowth of secondary tumors (1, 2). At each step, metastatic cells face multiple obstacles that are overcome with molecular alterations regulating the expression and function of specific metastasis-related genes (3).

Death-associated protein kinase (DAPK) is a metastasis suppressor. DAPK expression inhibits metastasis of Lewis lung carcinoma by increasing the sensitivity of tumor cells to programmed cell death (4). In addition, DAPK suppresses cell–matrix adhesion by inactivating integrin β1 (5), thereby inhibiting tumor cell motility (6). In line with the antimetastasis function of DAPK, clinical studies indicate that loss of DAPK expression in several cancer types is associated with advanced tumor stages and aggressive phenotypes, including metastasis (7). Although hypermethylation of *DAPK* promoter is frequently documented as an inactivation mechanism in tumors, loss of DAPK expression in the absence of promoter hypermethylation has also been reported (7), suggesting the existence of additional layer of DAPK regulatory mechanism in tumors.

The zinc finger transcriptional factor Krüppel-like factor 4 (KLF4) is expressed in several types of epithelial tissues. In the intestine, KLF4 expression is enriched in terminally differentiated epithelial cells near the luminal surface and gradually decreases toward the base of crypts (8). Conditional deletion of the *klf4* gene in the intestine leads to increased proliferation and migration and decreased differentiation of epithelial cells (9). In line with the maintenance of epithelial homeostasis of

Authors' Affiliations: [1]Institute of Biological Chemistry, Academia Sinica; [2]Institute of Biochemical Sciences, College of Life Science, National Taiwan University; [3]Division of Colorectal Surgery, Department of Surgery, National Taiwan University Hospital, Taipei; [4]Department of Biological Science and Technology, Institute of Bioinformatics and System Biology, National Chiao Tung University, Hsinchu, Taiwan; and [5]Division of Biomedical Sciences, University of California-Riverside, Riverside, California

Note: Supplementary data for this article are available at Cancer Research Online (http://cancerres.aacrjournals.org/).

H.-Y. Chen and Y.-M. Lin are the co-first authors.

J.-T. Liang and R.-H. Chen are co-senior authors.

Corresponding Author: Ruey-Hwa Chen, Institute of Biological Chemistry, Academia Sinica, 128 Academia Rd., Sec II, Nankang, Taipei, Taiwan 115. Phone: 8862-27855696, ext 6020; Fax: 8862-27889759; E-mail: rhchen@gate.sinica.edu.tw

doi: 10.1158/0008-5472.CAN-12-0667

Published OnlineFirst May 16, 2012; DOI: 10.1158/0008-5472.CAN-12-0667

the gastrointestinal tract, KLF4 displays a tumor suppressive function (10–12) and serves as a prognostic predictor for the survival of patients with gastrointestinal cancer (11, 13). Accordingly, *klf4* heterozygous deletion increases intestinal tumor burden in Apc^{Min} mice model (14). In colorectal cancer (CRC) cell line, KLF4 overexpression reduces transformation, migration, invasion, and tumorigenicity (15). Furthermore, KLF4 promotes epithelial traits by inducing the expression of several epithelial markers (16, 17) and suppressing tumor metastasis *in vivo* (18). Although KLF4 protein downregulation is prevalent in CRC (13), promoter hypermethylation and loss of heterozygosity of *klf4* are detected only in a small subset of CRC specimens (12), suggesting the existence of additional mechanism for KLF4 downregulation.

miRNAs are noncoding RNAs of 18 to 24 nucleotides that inhibit translation or induce mRNA decay through binding to the 3′-untranslated region (3′-UTR) of their target RNAs (19, 20). A number of miRNAs have been identified to regulate tumor metastasis (21, 22). Among them, miR-103 and miR-107, belonging to the miR-103/107 family due to their identical seed sequences, are capable of inducing epithelial-to-mesenchymal transition (EMT) of mammary epithelial cells, thereby fostering invasive and metastatic behaviors of breast cancers (23). This function of miR-103/107 is attributed to its suppression of Dicer. However, studies in CRC revealed that high expression of Dicer is associated with high-grade tumor and poor prognosis (24, 25). Thus, it remains unclear whether miR-103/107 act as metastamirs in CRC.

We report here that miR-103/107 target DAPK and KLF4 to potentiate cell–matrix adhesion and to inhibit cell–cell adhesion, thereby conferring motility and invasiveness of CRC cells. This miR-103/107–dependent regulation acts pleiotropically to potentiate CRC metastasis *in vivo*. Furthermore, a signature of miR-103/107 high, DAPK low, and KLF4 low expression profile correlates with metastasis, metastasis recurrence, and poor overall survival in patients with CRC. Our study reveals a pivotal role of miR-103/107–dependent DAPK and KLF4 modulation in CRC metastasis.

Materials and Methods

Materials

Plasmids, miRNAs, antagomiRs, antibodies, and other reagents are described in the Supplementary Materials and Methods.

Cell culture and transfection

All cell lines were obtained from American Type Culture Collection and used within 6 months of thawing. HCT116, HT29, SW620, and WiDr cells were cultured in RPMI-1640 medium containing 10% fetal calf serum (FCS). SW480 and CaCo-2 cells were maintained in Dulbecco's Modified Eagle's Medium (DMEM) containing 10% FCS and DMEM high glucose containing 10% FCS, respectively. Transfection was carried out by Lipofectamine 2000 Reagent (Invitrogen). Hypoxia experiments were carried out by placing cells in a closed chamber flushed with 1% O_2/5% CO_2/94% N_2.

In situ hybridization and immunohistochemical analysis

Tissue microarray containing 89 CRC specimens were obtained from Biomax Inc. and Pantomics Inc. In addition, 99 CRC specimens with survival and recurrence information were obtained from National Taiwan University Hospital Tissue Bank. Studies involving these tissues were approved by the Institutional Review Boards at College of Medicine, National Taiwan University and Academia Sinica (Taipei, Taiwan). *In situ* hybridization (ISH) analysis with 3′ DIG–labeled miRNA-103 LNA and miR-107 LNA and immunohistochemical analysis with avidin-biotin-peroxidase method are described in the Supplementary Materials and Methods.

Lentivirus production and infection

To generate recombinant lentivirus, 293FT cells were cotransfected with the package, envelop, and various expressing constructs. The virus-containing supernatant was harvested and concentrated by ultracentrifugation. For infection, the viral stock was supplemented with 8 μg/mL of polybrene.

Flow cytometric analysis

To assess cell surface expression of integrin, cells were washed with PBS, trypsinized by dissociation buffer (GIBCO), and resuspended in blocking solution (Ca^{2+}, Mg^{2+}-free HBSS containing 2% goat serum). Cells were then incubated with anti-integrin β1 antibody HUTS-21 or P5D2 for 1 hour at 4°C, washed with PBS, and labeled with secondary antibody for 30 minutes at 4°C. Cells were washed and analyzed on a Becton Dickinson FACScan flow cytometer.

Luciferase assay

For 3′-UTR analysis, cells were cotransfected with psi-CHECK-2–based construct and pre-miR-103/107 or a negative control. Luciferase assay was conducted with the Dual-Luciferase Reporter Assay System (Promega).

Cell migration and invasion

For migration assay, the underside of Transwell polycarbonate membrane was coated with fibronectin. Cells resuspended in 10% FCS medium containing 1% bovine serum albumin (BSA) were plated onto the upper chamber, and the medium containing 1% BSA and 20% FCS was added to the lower chamber. Cells were incubated at 37°C under normoxia or hypoxia conditions. At the end point of incubation, cells that had migrated onto the lower membrane surface were fixed by 4% formaldehyde and counted. For invasion assay, the Transwell membrane was coated with Matrigel.

Cell adhesion

Cells resuspended in RPMI medium containing 1% BSA were plated on wells precoated with 10 μg/mL (for HT29) or 20 μg/mL (for HCT116) of fibronectin and incubated for 20 to 40 minutes at 37°C. Nonadherent cells were removed and attached cells were fixed with 3.7% paraformaldehyde and stained with 0.1% crystal violet.

Calcium switch

For analyzing junctional reassembly, cells were treated with medium containing 1 mmol/L EGTA at 37°C for 2 hours,

Published OnlineFirst May 16, 2012; DOI: 10.1158/0008-5472.CAN-12-0667

followed by incubation in calcium-containing medium for 1 or 3 hours at 37°C. The cells were fixed and stained with anti-E-cadherin antibody and 4′, 6-diamidino-2-phenylindole (DAPI). The images were captured with a confocal microscope (510 Meta; Carl Zeiss MicroImaging Inc.) equipped with a ×63 oil objective lens.

Anoikis assay

Cells were seeded on plates precoated with 0.1 μg/mL of fibronectin and cultured for 14 hours. For all apoptosis-related assays, both detached and adherent cells were harvested and combined. DNA fragmentation was measured by Cell Death ELISA Kit (Roche).

In vivo models

Seven-week-old male Swiss *nu*/*nu* mice were purchased from National Laboratory Animal Center, Taipei, Taiwan and were housed and maintained under specific pathogen-free conditions. All mouse experiments were conducted with approval from the Experimental Animal Committee, Academia Sinica. For orthotopic transplantation, cells were resuspended (2×10^6 cells/0.05 mL HBSS) and injected into the wall of the cecum. Local invasion was examined at week 4, whereas liver metastasis and primary tumor growth were at week 8 after implantation. For experimental metastasis, cells tagged with luciferase using lentiviral transduction were resuspended (1×10^6 cells/0.05 mL PBS) and injected into the tail vein. Lung metastasis was monitored by bioluminescent imaging using IVIS image system. Seven weeks later, mice were killed for examining lung metastasis.

Results

miR-103/107 expression correlates with CRC metastasis and poor survival

To investigate the roles of miR-103 and miR-107 in CRC metastasis, we examined their expression in a panel of CRC cell lines showing differential metastasis potential in an orthotopic model (26–30). Using qPCR analysis with primers specific to miR-103 and miR-107 (Supplementary Fig. S1A), we observed positive correlations between the levels of miR-103 and miR-107 and the metastasis potential of these cells (Fig. 1A). Because the 2 miRNAs are expected to elicit similar biologic functions due to their identical seed sequences, their combinatory expression level and effect were analyzed in the subsequent studies. We conducted ISH analysis of miR-103/107 expressions in a cohort of 188 human CRC specimens. Representative images are presented in Fig. 1B. Remarkably, miR-103/107 expression was elevated in stage III compared with stage II tumors (Supplementary Table S1), and high expression of miR-103/107 was associated with lymph node metastasis (N1–N3) and distant metastasis (M1; Table 1). Kaplan–Meier analysis on patients with survival data ($n = 99$) revealed that miR-103/107 high expression correlated with metastatic recurrence and poor overall survival (Fig. 1C). Our results indicate miR-103/107 as a marker of poor prognosis of CRC and suggest a metastasis-promoting function of these 2 miRNAs in CRC.

miR-103/107 target DAPK and KLF4 in CRC cells

miR103/107 was reported to promote EMT and metastasis in breast cancers by targeting Dicer (23). In CRC, however, Dicer expression is augmented in high-grade tumor and predicts poor survival (24, 25), which do not support a major role of Dicer in CRC metastasis. To identify potential targets of miR-103/107 in CRC, we used miRanda (31) and TargetScan (32) algorithms. Candidates recovered from these algorithms were analyzed by Cancer Gene Index (https://wiki.nci.nih.gov/display/cageneindex/Cancer+Gene+Index+End+User+Documentation) to search for metastasis suppressors. Among them, we were particularly interested in DAPK, KLF4, and PTEN, because they all elicit a metastasis-suppressive function (4, 18, 33). We examined the effect of miR-103/107 on the expression of these 3 candidates in CRC cell lines. Overexpression of miR-103/107 in HCT116 cells reduced the protein levels of DAPK and KLF4 but not PTEN (Fig. 2A). Downregulation of DAPK and KLF4 by miR-103/107 was recapitulated in another CRC cell line, DLD-1. miR-103/107, however, did not affect *DAPK* and *KLF4* mRNA levels (Supplementary Fig. S1B). To investigate whether endogenous miR-103/107 could regulate endogenous DAPK and KLF4, we transfected HCT116 cells with antagomiR-103/107, which blocked the function of miR-103/107 (Supplementary Fig. S2). AntagomiR-103/107 induced a concurrent elevation of DAPK and KLF4, which was reversed by DAPK and KLF4 siRNAs, respectively (Fig. 2B). To substantiate that *DAPK* and *KLF4* are direct targets of miR-103/107, we generated reporter constructs in which the full-length 3′-UTR of *DAPK* or *KLF4* was cloned downstream of the luciferase open reading frame. Overexpression of miR-103/107 reduced the activities of *DAPK*- and *KLF4*-based reporters, whereas antagomiR-103/107 markedly increased the activities of 2 reporters (Fig. 2C and D). Furthermore, mutagenesis of the seed sequences of predicted miR-103/107–binding sties on *DAPK* 3′-UTR abrogated the responsiveness to miR-103/107 (Fig. 2C). In the case of *KLF4* 3′-UTR, 2 putative miR-103/107–binding sites were found and they functioned cooperatively to suppress the reporter activity (Fig. 2D). In line with the results of reporter assays, the expressions of Flag-DAPK and Flag-KLF4 from constructs that lack 3′-UTR sequences were not affected by miR-103/107 (Fig. 2E). These results indicate that miR-103/107 suppress the expression of DAPK and KLF4 by targeting their 3′-UTRs.

The signature of miR-103/107 high, DAPK low, and KLF4 low expression correlates with metastasis and poor prognosis of CRC patients

To evaluate the clinical relevance of miR-103/107–induced downregulation of DAPK and KLF4, we conducted immunohistochemical analysis for DAPK and KLF4 expression in CRC specimens derived from consecutive slides that had been analyzed for miR-103/107 expression. Representative images from a metastatic case and a nonmetastatic case are presented in Fig. 1D. This analysis revealed that miR-103/107 expression correlated inversely with DAPK and KLF4 expression (Fig. 1E), suggesting the existence of

Published OnlineFirst May 16, 2012; DOI: 10.1158/0008-5472.CAN-12-0667

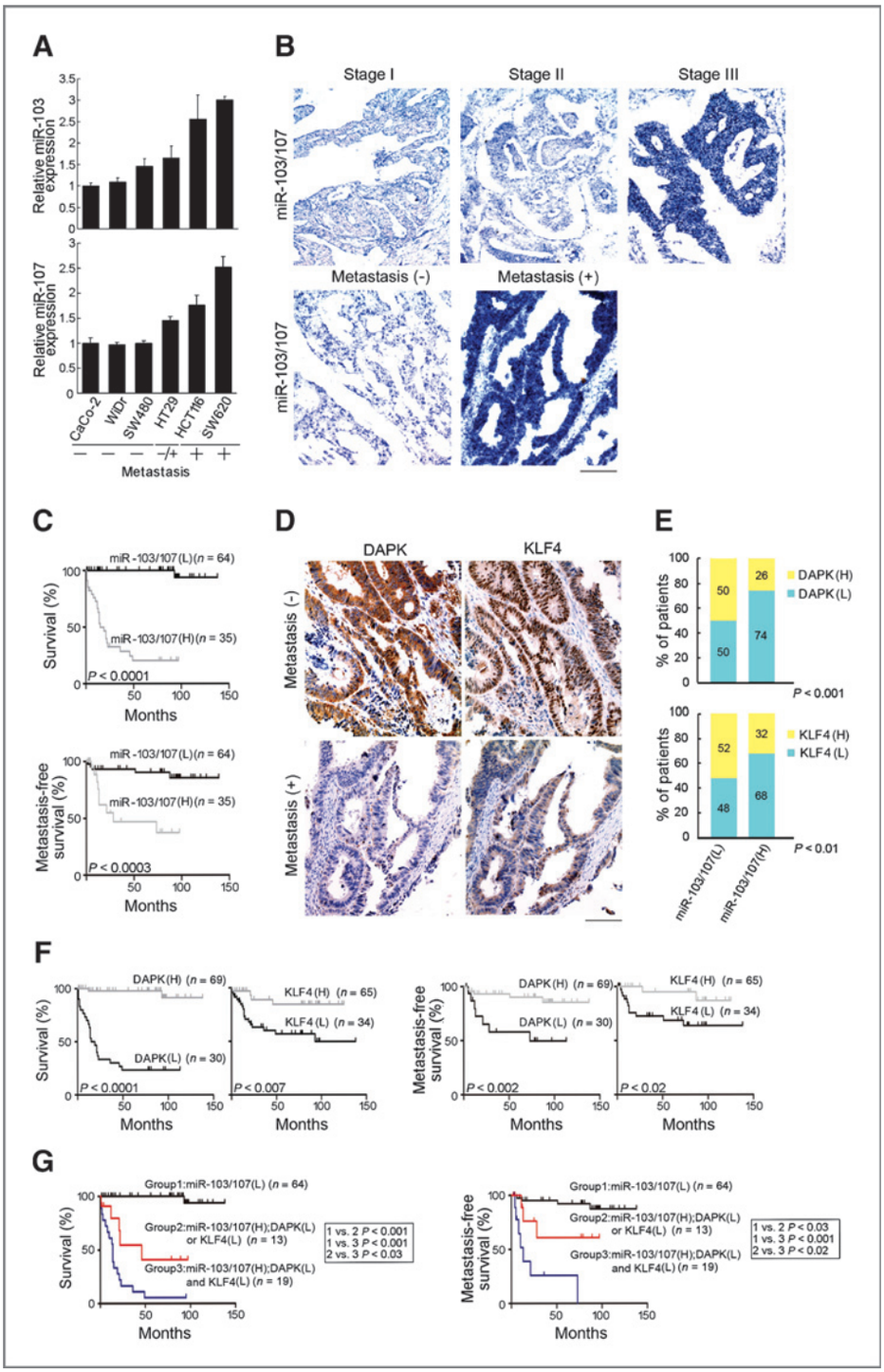

Figure 1. The expression profile of miR-103/107 high, DAPK low, and KLF4 low correlates with metastasis and poor survival of patients with CRC. A, reverse transcription/quantitative polymerase chain reaction analysis of miR-103 and miR-107 expression in CRC cell lines. Data are mean ± SD, $n = 3$. B and D, representative ISH staining for miR-103/107 (B) and immunohistochemical staining for DAPK and KLF4 (D) in primary tumors from indicated classes of patients with CRC. Bars, 200 μm. E, inverse correlation of miR-103/107 expression with DAPK or KLF4 expression in 188 CRC specimens. Fisher exact test was used for comparison between groups. C, F, and G, Kaplan–Meier analysis of overall survival and metastasis-free survival of patients with CRC with the corresponding expression profiles (C and F), and subgroup analysis of CRC cases according to the expression profile of miR-103/107, DAPK, and KLF4 (G). The 3 patients displaying miR-103/107 high, DAPK high, and KLF4 high expression were omitted in G.

miR-103/107–dependent modulation of DAPK and KLF4 in this cohort of patients. Similar to miR103/107 upregulation, DAPK and KLF4 downregulation was each associated with metastasis to lymph node and distant organs (Table 1), as well as with a shorter metastasis-free period and reduced overall survival (Fig. 1F). More importantly, patients with a miR-103/107 high, DAPK low, and KLF4 low expression signature had the shortest metastasis-free period and the worst overall survival (Fig. 1G). The prognostic significance of this expression signature was showed by multivariate analysis and was independent of other prognostic markers, such as T stage and N stage (Supplementary Table S2). These

Published OnlineFirst May 16, 2012; DOI: 10.1158/0008-5472.CAN-12-0667

Table 1. The miR-103/107, DAPK, and KLF4 expression profiles with relation to metastasis

Clinicopathologic parameters	Cases no.	miR-103/107 expression			DAPK expression			KLF4 expression		
		Low (%)	High (%)	*P*	Low (%)	High (%)	*P*	Low (%)	High (%)	*P*
Node status										
N0	87	52 (60)	35 (40)		43 (49)	44 (51)		40 (46)	47 (54)	
N1–N3	101	36 (36)	65 (64)	<0.002	75 (74)	26 (26)	<0.0006	70 (69)	31 (31)	<0.002
Distant metastasis										
M0	159	81 (51)	78 (49)		94 (59)	65 (41)		87 (55)	72 (45)	
M1	29	7 (24)	22 (76)		24 (83)	5 (17)		23 (79)	6 (21)	<0.02

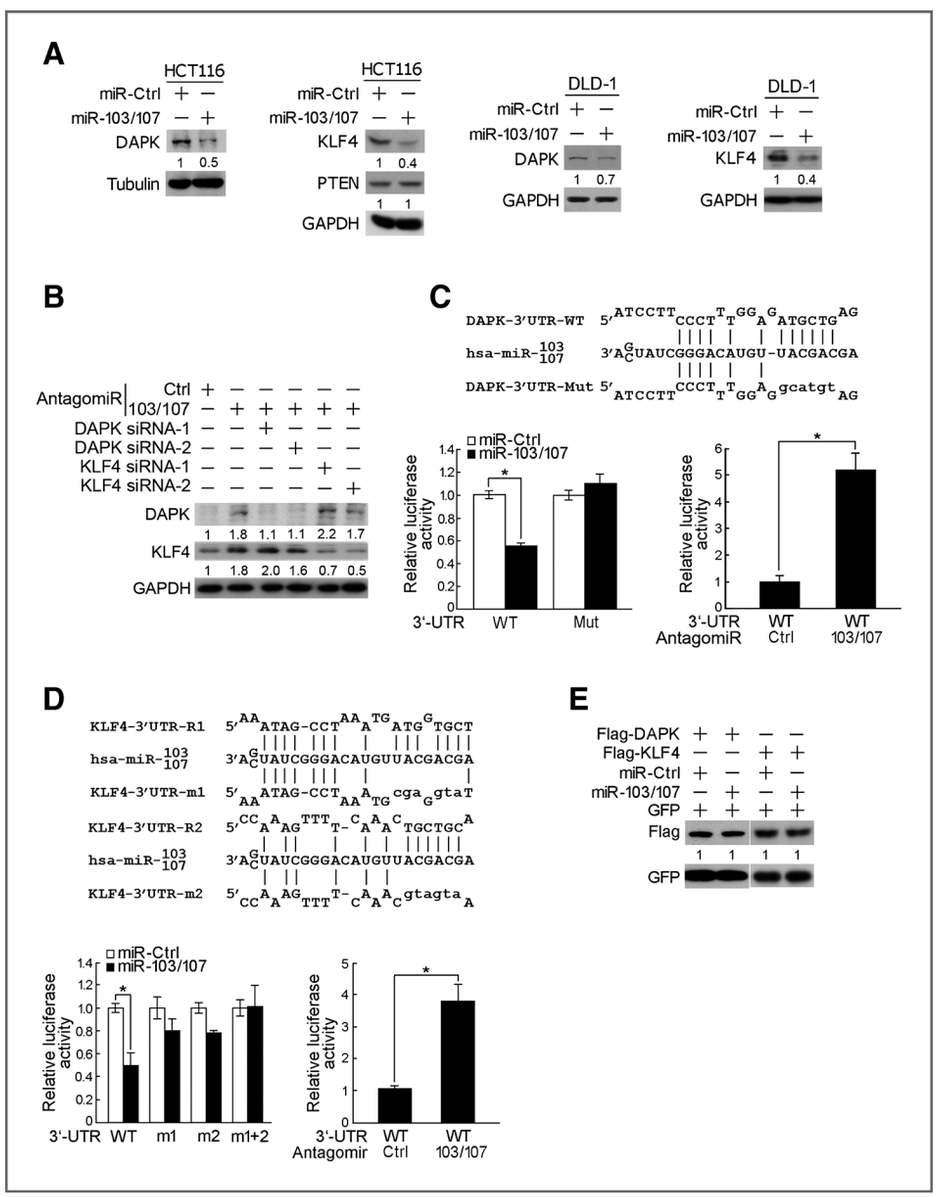

Figure 2. miR-103/107 target DAPK and KLF4. A, immunoblot analysis of HCT116 and DLD-1 cells transfected with indicated miRNAs. B, immunoblot analysis of HCT116 cells transfected with indicated antagomiRs or siRNAs. C and D, predicted sequences of the miR-103/107–binding sites within the 3′-UTR of *DAPK* and *KLF4* and the sequences of *DAPK* and *KLF4* 3′-UTR mutants (Mut) used in this study (top). Luciferase activity in HCT116 cells upon transfection of indicated 3′-UTR–driven reporter constructs and miRNAs or antagomiRs. E, immunoblot analysis of HCT116 cells transfected with indicated constructs and GFP. All numerical data are mean ± SD. *, $P < 0.05$, $n = 3$. GAPDH, glyceraldehyde-3-phosphate dehydrogenase; WT, wild-type.

Published OnlineFirst May 16, 2012; DOI: 10.1158/0008-5472.CAN-12-0667

data support that miR-103/107–dependent regulation of DAPK and KLF4 is associated with metastasis and poor prognosis of patients with CRC.

DAPK and KLF4 mediate miR-103/107–induced motility and invasiveness in CRC cells

The strong association of the expression profile of miR-103/107, DAPK, and KLF4 with CRC metastasis prompted us to investigate the impacts of miR-103/107–dependent regulation of DAPK/KLF4 on metastasis-relevant traits. To this end, HT29 cells stably expressing miR-103/107, DAPK, and/or KLF4 were established (Fig. 3A, left). miR-103/107 overexpression induced a significant increase in motility and invasiveness, which was partially suppressed by reexpression of DAPK or KLF4 (Fig. 3A, middle and right). Similar findings were observed with another CRC cell line, HCT116 (Supplementary Fig. S3). Notably, immunoblot analysis confirmed miR-103/107–induced downregulation of DAPK and KLF4 in these cell lines, which were rescued by reexpression of DAPK and KLF4, respectively (Fig. 3A and Supplementary Fig. S3, left). In a reciprocal experiment, antagomiR-103/107 inhibited migration and invasion of HCT116 cells. More importantly, these effects were partially reversed by silencing of either DAPK or KLF4 and completely abrogated by depletion of both (Fig. 3B). Thus, concurrent repression of DAPK and KLF4 plays a major role in miR-103/107–induced CRC cell migration and invasion.

Hypoxia is an essential feature of tumor microenvironments and is associated with the development of metastasis (34). Because previous (35) and present (Supplementary Fig. S4) studies showed that miR-103 and miR-107 levels are elevated in hypoxia, we investigated whether hypoxia reduces the expression of DAPK and KLF4 through miR-103/107 and whether this miR103/107–induced regulation contributes in part to hypoxia-stimulated migration and invasion. Indeed, we found that DAPK and KLF4 were downregulated

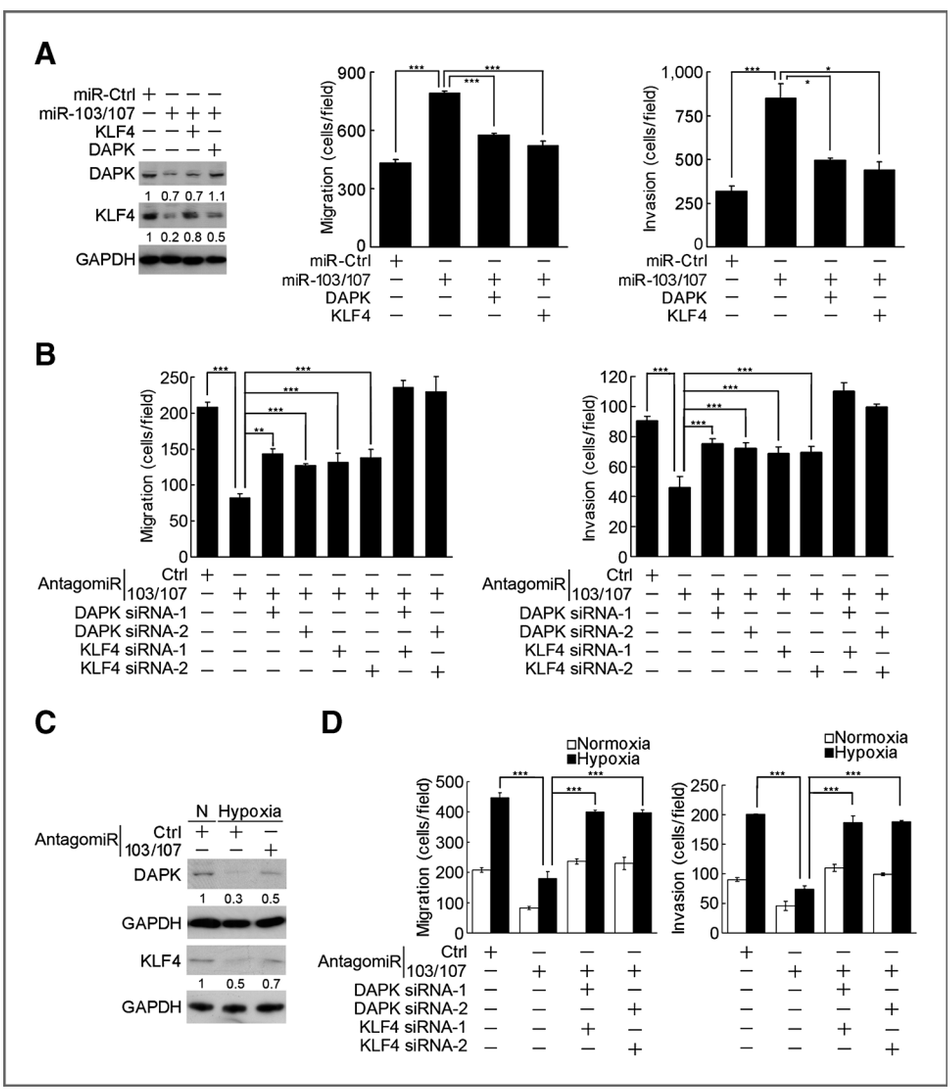

Figure 3. Repression of DAPK and KLF4 mediates miR-103/107–induced motility and invasiveness in normoxic and hypoxic cells. A, immunoblot analysis and migration/invasion assays of HT29 cells stably expressing indicated miRNAs and/or cDNAs. B, HCT116 cells as in Fig. 2B were assayed for migration and invasion. C, immunoblot analysis of HCT116 cells transfected with indicated antagomiRs and cultured in hypoxia or normoxia for 48 hours. D, HCT116 cells transfected with indicated antagomiRs and/or siRNAs were cultured in normoxia or hypoxia for 16 hours and assayed for migration and invasion. All numerical data are mean ± SD. $^{*}, P < 0.05$; $^{***}, P < 0.0005, n \geq 3$. GAPDH, glyceraldehyde-3-phosphate dehydrogenase.

Published OnlineFirst May 16, 2012; DOI: 10.1158/0008-5472.CAN-12-0667

in response to hypoxia and antagomiR-103/107 rescued their expression in hypoxic cells (Fig. 3C). Furthermore, antagomiR-103/107 drastically reduced migration and invasion of hypoxic HCT116 cells, and these effects were completely abrogated by depletion of both DAPK and KLF4 (Fig. 3D). Collectively, our data support a crucial and physiologic role of miR-103/107–dependent DAPK and KLF4 repression in CRC cell motility and invasiveness under both normoxia and hypoxia conditions.

miR-103/107–mediated suppression of DAPK and KLF4 promotes cell–matrix adhesion and inhibits cell–cell adhesion

We next investigated the underlying mechanisms through which miR103/107–dependent regulation of DAPK and KLF4 potentiates CRC cell motility and invasiveness. Our previous study revealed that DAPK suppresses cell–matrix adhesion through inactivating integrin β1 (5). Because cell motility is greatly influenced by cell–matrix adhesion, we evaluated the effect of miR-103/107 on cell attachment to fibronectin. We found that miR-103/107 overexpression in HT29 and HCT116 cells led to a significant increase in cell–matrix adhesion and this effect was reversed by reexpression of DAPK (Fig. 4A). In line with this finding, miR-103/107 prevented cell death induced by low matrix concentrations (anoikis) and reexpression of DAPK abolished this function (Fig. 4B). Furthermore, ectopic miR-103/107 stimulated integrin β1 activity without affecting its abundance and DAPK reexpression again abolished this integrin-regulating function (Fig. 4C). Consistent with the enhanced cell–matrix adhesion, the migration-promoting effect of miR-103/107 was more pronounced under low matrix concentrations (Supplementary Fig. S5A). In addition to cell–matrix adhesion, cell–cell adhesion also plays a crucial role in regulating cell motility. Notably, KLF4 induces the expression of several epithelial markers that contribute to cell–cell adhesion, such as E-cadherin, claudin-3, and occludin (16, 17). Accordingly, overexpression of miR-103/107 in HT29 and SW480 cells decreased the expression of these epithelial markers and reexpression of KLF4 at least partially recovered their expression (Fig. 4D and Supplementary

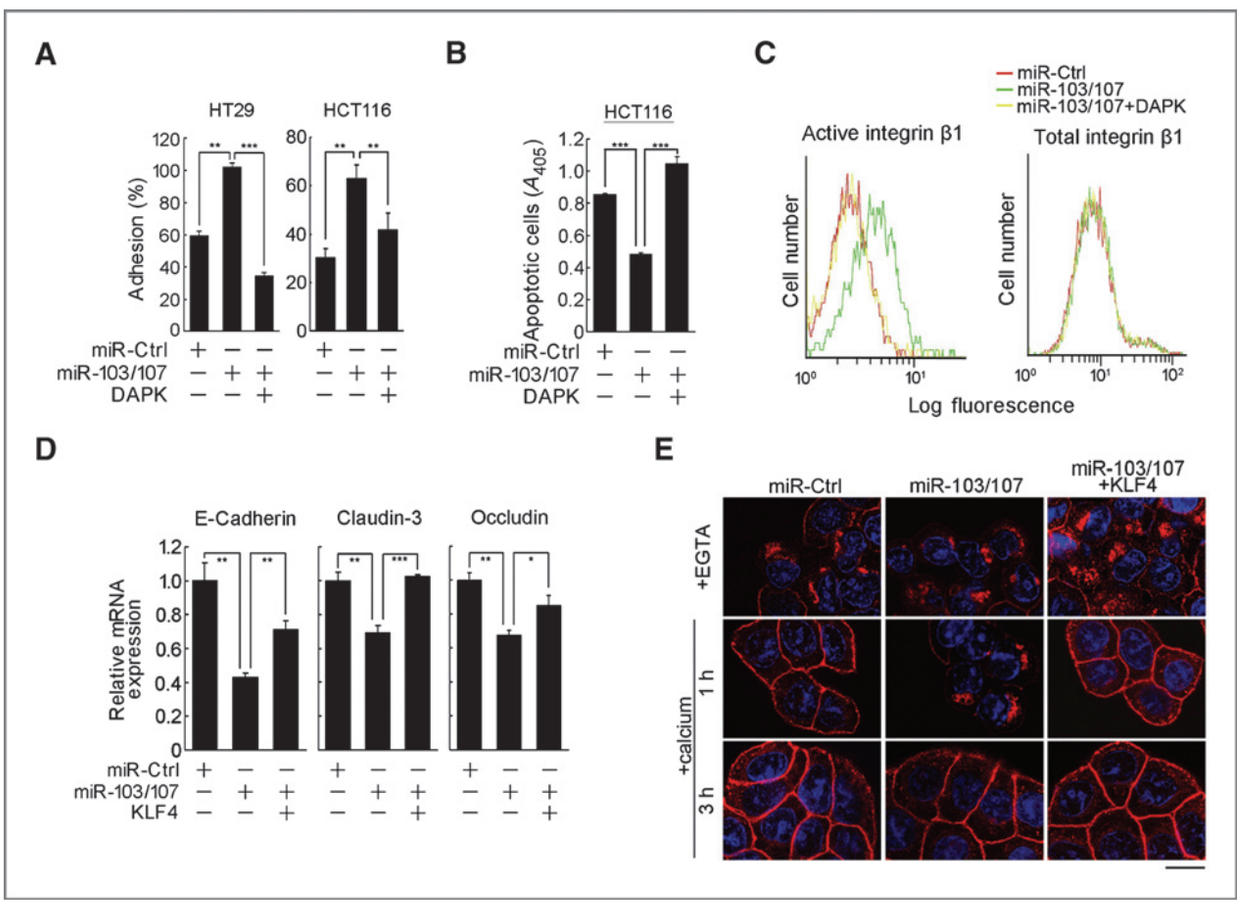

Figure 4. miR-103/107–induced repression of DAPK and KLF4 potentiates cell–matrix adhesion and diminishes cell–cell adhesion. A and B, HT29 or HCT116 cells transfected with indicated constructs were assayed for adhesion on fibronectin for 25 minutes (A) or for anoikis (B). C, cell surface expression of active or total integrin β1 in HT29 cells transfected with indicated constructs was assayed by flow cytometric analysis. D, HT29 cells transfected with indicated constructs were assayed for the expression of indicated genes by RT/qPCR. E, adherens junction assembly assay. HT29 cells stably expressing miR-103/107 together with or without KLF4 were cultured in indicated conditions and stained with anti-E-cadherin antibody (red) and DAPI (blue). Bar, 10 μm. All numerical data are mean ± SD. *, $P < 0.05$; **, $P < 0.005$; ***, $P < 0.0005$, $n \geq 3$.

Published OnlineFirst May 16, 2012; DOI: 10.1158/0008-5472.CAN-12-0667

Fig. S5B and S5C). miR-103/107, however, did not affect the expression of mesenchymal markers Slug and Snail (Supplementary Fig. S5D), which is consistent with the reported function for KLF4 (16). In line with the downregulation of epithelial markers without affecting the expression of mesenchymal markers, miR-103/107 overexpression was insufficient to induce EMT in a number of CRC cell lines (Supplementary Fig. S5E). However, when tested for the formation of adherens junctions by the calcium switch methodology (see Materials and Methods), we found that miR-103/107 caused a significant delay in the assembly of E-cadherin–mediated adhesions (Fig. 4E) and this effect was again abolished by KLF4 reexpression (Fig. 4E). Thus, our study showed that miR-103/107 repress DAPK and KLF4 to promote a number of metastasis-relevant traits *in vitro*, including stimulating migration, invasion, and cell–matrix adhesion and suppressing epithelial marker expression and adherens junction assembly.

Reexpression of DAPK and KLF4 reverses miR-103/107–imposed metastasis *in vivo*

We next investigated the impact of miR-103/107–dependent DAPK and KLF4 repression on CRC metastasis using a well-established orthotopic model (26–30). To this end, HCT116 derivatives (see Supplementary Fig. S3) were injected into the cecum of nude mice. These cell lines exhibited comparable proliferation rates *in vitro* (Supplementary Fig. S6A). However, at 8 weeks after implantation, we found that miR-103/107 overexpression significantly increased the size and number of metastatic nodules in the liver, and this effect was partially suppressed by reexpression of DAPK or KLF4 (Fig. 5A and B). Primary tumor weight, tumor cell proliferation rate, and angiogenesis at the primary site, however, were not significantly differed among the 4 groups (Fig. 5C and D and Supplementary Fig. S6B and S6C). Histologic analysis of tissues adjacent to the

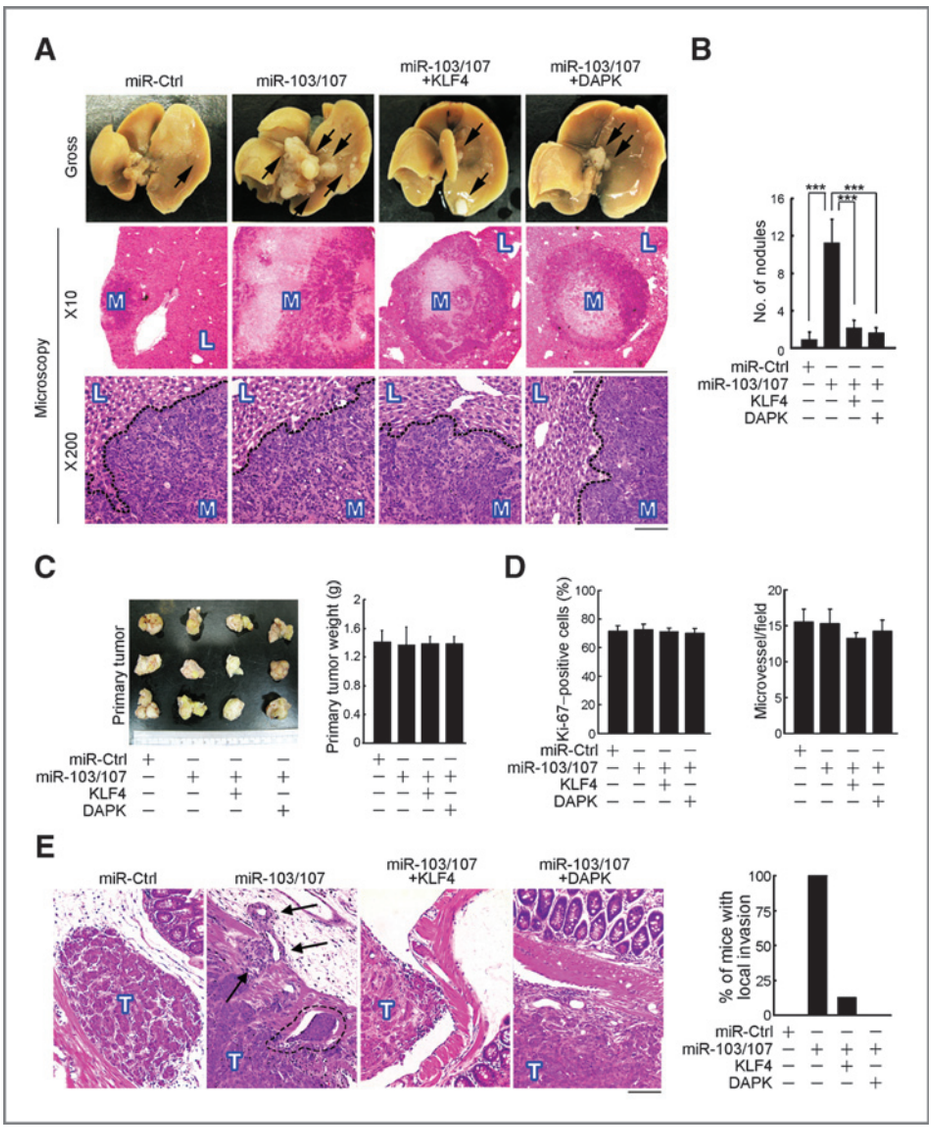

Figure 5. miR-103/107–dependent regulation of DAPK and KLF4 potentiates CRC local invasion and metastasis in an orthotopic mouse model. A, liver metastasis and histologic analysis of liver from mice at 8 weeks after implantation of indicated tumor cell lines. The metastatic nodules in liver are indicated by arrows (top). The low-magnitude view shows the size of nodules (middle), whereas the high-magnitude image reveals the histologic characters of tumor cells (bottom). M, Metastatic nodules; L, Liver. Bars, 1 mm (middle) and 200 μm (bottom). B, the numbers of metastatic nodules in liver per mouse. C, primary tumors derived from indicated cells at 8 weeks after implantation. Average tumor weight is indicated on the right. D, quantitative data of Ki-67 (left) and CD31 (right) staining of primary tumors derived from indicated cells. E, the percentage of mice showing local invasion and histologic analysis of tissues adjacent to primary tumors at 4 weeks after orthotopic implantation. The miR-103/107–bearing tumor showed tumor cells invasion through muscle layers (arrows) and vascular invasion (dashed circle). T, tumor. Bar, 200 μm. All numerical data are mean ± SD. ***, $P < 0.0005$, $n = 6$.

Published OnlineFirst May 16, 2012; DOI: 10.1158/0008-5472.CAN-12-0667

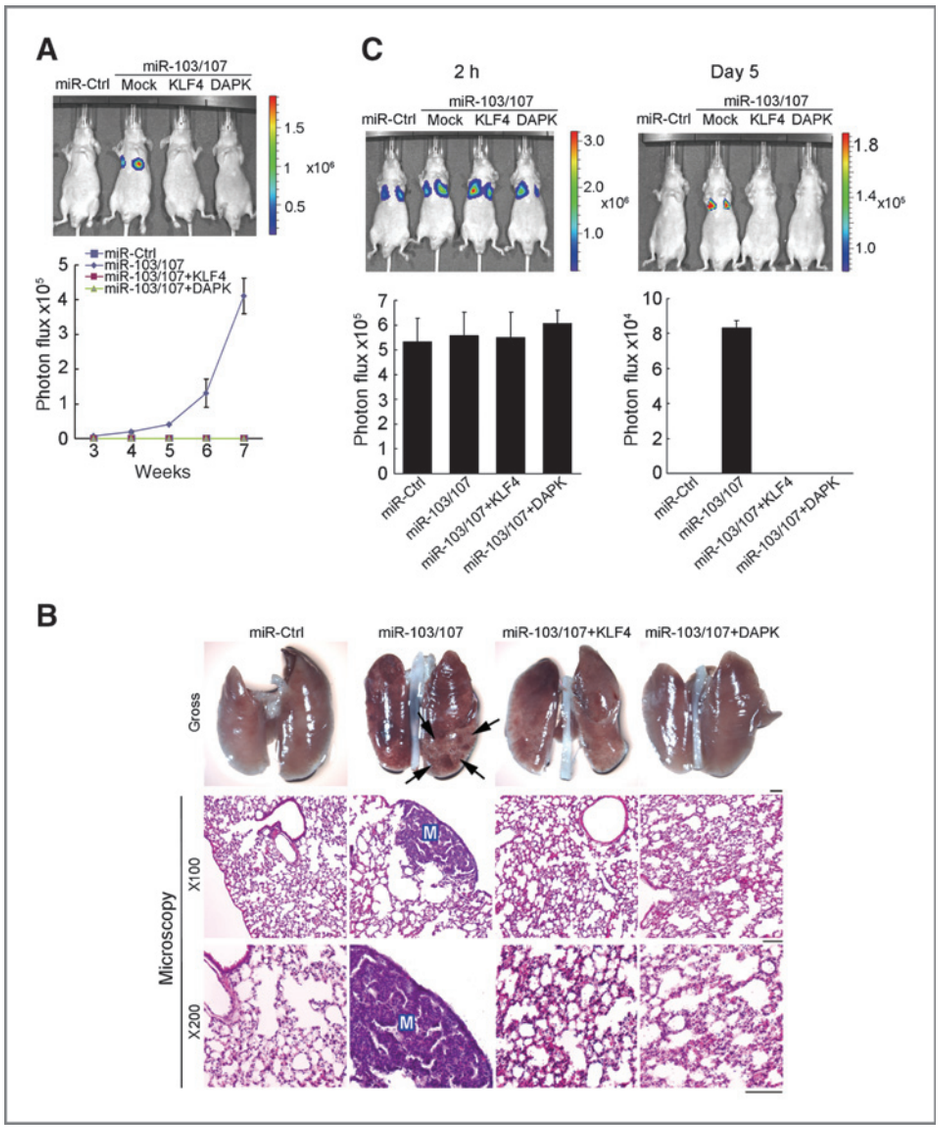

Figure 6. miR-103/107–dependent regulation of DAPK and KLF4 potentiates colonization of CRC cells in metastatic site. A, bioluminescence analysis and quantification of lung metastasis. Representative images at week 7 (top) and the kinetic of metastasis at indicated time points (bottom) after injection are shown. B, lung metastatic nodules (top) and histologic analysis of lung (bottom) at week 7. Metastatic nodules are indicated by arrows (top) and "M" (middle, bottom). Bars, 1 mm (top); 200 μm (middle, bottom). C, bioluminescence analysis of kinetics of metastasis of indicated cells. Data are mean ± SD. $n = 6$ (A and B) and $n = 4$ (C).

primary tumors at 4 weeks after implantation revealed that miR-103/107–expressing cells generated tumors with high local invasion capability, whereas tumors derived from parental HCT116 cells did not show sign of invasion (Fig. 5E). The miR-103/107–stimulated local invasion was suppressed by reexpression of DAPK or KLF4. These data indicate that miR-103/107 target DAPK and KLF4 to potentiate CRC liver metastasis and this activity is mediated at least in part through the stimulation of local invasion.

To determine whether miR-103/107–induced downregulation of DAPK and KLF4 also influenced on later steps of the metastasis process, the aforementioned HT29 derivatives (see Fig. 3A) were injected directly into circulation of mice, thereby circumventing local invasion and intravasation. Remarkably, while miR-103/107–bearing cells developed lung metastases as early as 3 to 4 weeks after injection, control cells or cells coexpressing miR-103/107 together with DAPK or KLF4 did not generate lung metastasis even at 7 weeks after injection (Fig. 6A and B). Bioluminescence imaging analysis at 2 hours after injection revealed that the 4 groups of cells displayed comparable ability to arrive lung vasculature (Fig. 6C). However, at 5 days after injection, while the miR-103/107–bearing cells could still be detected in the lung, the other 3 groups did not show bioluminescence signal, suggesting their inability to persist in the lung. These data support that miR-103/107–mediated repression of DAPK and KLF4 promotes CRC colonization at metastatic sites.

Discussion

We identify miR-103/107 as prometastatic miRNAs in CRC and negative regulators of 2 metastasis suppressors, DAPK and KLF4. Through concurrent repression of DAPK

Published OnlineFirst May 16, 2012; DOI: 10.1158/0008-5472.CAN-12-0667

and KLF4, miR-103/107 inactivate integrin β1 to promote cell–matrix interaction and downregulate E-cadherin/claudin-3/occludin to diminish cell–cell adhesion, which could act in concert to increase cell motility. Although downregulation of E-cadherin, claudin-3, and occludin is insufficient to induce EMT *in vitro*, it likely sensitizes tumor cells to EMT-inducing signals arising from tumor microenvironments, thereby promoting local invasion *in vivo*. In addition, the suppression of DAPK is expected to facilitate evasion of apoptosis or anoikis during several steps of metastatic progression. Thus, the concomitant repression of DAPK and KLF4 by miR-103/107 could potentiate metastasis by regulating multiple stages of the invasion-metastasis cascade. In support of this notion, miR-103/107 overexpression increases local invasion and liver metastasis in a CRC orthotopic model as well as colonization in the distant metastatic site in an experimental metastasis model. More importantly, all of these effects are reversed at least partially by reexpression of DAPK or KLF4. Our study thus indicates a critical and pleiotropic role of miR-103/107–dependent repression of DAPK and KLF4 in CRC metastasis.

The induction of miR-103/107 and concomitant downregulation of DAPK and KLF4 in hypoxia further highlights the importance of this regulatory circuit in tumor progression. Because hypoxia is a potent inducer of tumor metastasis, the induction of prometastatic miR-103/107 and suppression of antimetastatic DAPK and KLF4 may be part of the metastasis program elicited by hypoxic tumor microenvironments. In line with this notion, we show that miR-103/107–dependent modulation of DAPK and KLF4 contributes in part to hypoxia-stimulated motility and invasion. The frequent upregulation of HIF-1 in tumors may account for one mechanism underlying miR-103/107 overexpression in CRC. Importantly, this miR-103/107 upregulation correlates with DAPK and KLF4 downregulation and the concurrent miR-103/107 upregulation and DAPK and KLF4 downregulation correlates with lymph node and distant metastasis, metastatic recurrence, and poor overall survival. Thus, our findings underscore the clinical relevance and prognostic significance of miR-103/107–dependent DAPK/KLF4 regulation in CRC.

Hypermethylation of the *DAPK* promoter has been a major mechanism for DAPK downregulation in many types of human tumors (7). In CRC, however, conflicting results have been reported for the frequency of *DAPK* promoter methylation (36–38). Our previous study identified a tyrosine phosphorylation mechanism for DAPK inactivation, which is detected in a small portion of patients with CRC (39). In this study, our findings of miR-103/107–dependent DAPK downregulation and its correlation with CRC progression suggest this miRNA-mediated posttranscriptional regulation as a novel mechanism for suppressing DAPK in tumors. Similar to DAPK, KLF4 downregulation has been found in CRC. In addition to hypermethylation and loss of heterozygosity of the *KLF4* gene in CRC reported previously (10, 12), our study suggests miRNA-mediated modulation as an additional mechanism for KLF4 downregulation in CRC. Of note, besides miR-103/107, a recent study indicates that KLF4 is targeted by miR-10b to foster the migration and invasion of esophageal cancer cells (40). Nevertheless, KLF4 also possesses context-dependent oncogenic roles in certain tissues (41) and its expression correlates with B lymphoma Mo-MLV insertion region 1 homolog (BMI)-1–induced proliferation of endometrial cancer cells (42).

miRNAs possess the capacity to coordinately repress a cohort of RNAs by targeting their 3′-UTRs. Given that these targets can also be regulated by other mechanisms, it is conceivable to observe a tissue-specific or context-specific effect of miRNA. In line with this notion, miR-103/107 promote EMT in breast epithelial cells by repressing Dicer (23). This EMT effect, however, was not observed in multiple CRC cell lines in our study. In CRC, Dicer expression correlates with tumor progression and poor prognosis (24, 25), suggesting a tumor-promoting rather than tumor-suppressive role. Thus, the discrepancy of the effect of miR-103/107 on EMT in breast cancer and CRC might be attributed to a tissue-specific effect of Dicer. Likewise, a recent study reported that miR-107 potentiates tumor growth of breast cancer cells (43), which is in contrast to our finding that miR-103/107 fail to affect tumor growth. Despite the differences in tumor-promoting mechanisms, the capabilities of miR-103/107 to act on different tumor suppressors and to influence on distinct aspects of tumor progression in different cancer types underscore their functions as "oncomirs"

Disclosure of Potential Conflicts of Interest

No potential conflicts of interest were disclosed.

Authors' Contributions

Conception and design: R.-H. Chen, H.-Y. Chen, Y.-M. Lin, H.-C. Chung, Z. Chen, J. Y.-J. Shyy

Development of methodology: H.-Y. Chen, Y.-M. Lin, H.-C. Chung, Y.-D. Lang, C.-J. Lin, H.-D. Huang, J. Y.-J. Shyy

Acquisition of data (provided animals, acquired and managed patients, provided facilities, etc.): H.-Y. Chen, Y.-M. Lin, H.-C. Chung, Y.-D. Lang, C.-J. Lin, J. Huang, J.-T. Liang

Analysis and interpretation of data (e.g., statistical analysis, biostatistics, computational analysis): R.-H. Chen, H.-Y. Chen, Y.-M. Lin, H.-C. Chung, J. Huang, W.-C. Wang, F.-M. Lin, Z. Chen, H.-D. Huang

Writing, review, and/or revision of the manuscript: R.-H. Chen, H.-Y. Chen, Y.-M. Lin, H.-C. Chung, Z. Chen, J. Y.-J. Shyy

Administrative, technical, or material support (i.e., reporting or organizing data, constructing databases): Y.-D. Lang

Study supervision: R.-H. Chen

Acknowledgments

The authors thank Shu-Chun Teng and Pei-Wen Hsiao for reagents, Chin-Chun Hung for confocal analysis, and Taiwan Mouse Clinics for IVIS analysis.

Grant Support

The study was supported by Academia Sinica Investigator Award and National Science Council NSC 98-2320-B-001-021-MY3 (R.H. Chen) and UST-UCSD International Center of Excellence in Advanced Bioengineering sponsored by National Science Council I-RiCE Program NSC-100-2911-I-009-101 (H.D. Huang).

The costs of publication of this article were defrayed in part by the payment of page charges. This article must therefore be hereby marked *advertisement* in accordance with 18 U.S.C. Section 1734 solely to indicate this fact.

Received February 22, 2012; revised April 9, 2012; accepted May 7, 2012; published OnlineFirst May 16, 2012.

Published OnlineFirst May 16, 2012; DOI: 10.1158/0008-5472.CAN-12-0667

References

1. Fidler IJ, Yano S, Zhang RD, Fujimaki T, Bucana CD. The seed and soil hypothesis: vascularisation and brain metastases. Lancet Oncol 2002;3:53–7.
2. Nguyen DX, Bos PD, Massague J. Metastasis: from dissemination to organ-specific colonization. Nat Rev Cancer 2009;9:274–84.
3. Steeg PS. Tumor metastasis: mechanistic insights and clinical challenges. Nat Med 2006;12:895–904.
4. Inbal B, Cohen O, Polak-Charcon S, Kopolovic J, Vadai E, Eisenbach L, et al. DAP kinase links the control of apoptosis to metastasis. Nature 1997;390:180–4.
5. Wang WJ, Kuo JC, Yao CC, Chen RH. DAP-kinase induces apoptosis by suppressing integrin activity and disrupting matrix survival signals. J Cell Biol 2002;159:169–79.
6. Kuo JC, Wang WJ, Yao CC, Wu PR, Chen RH. The tumor suppressor DAPK inhibits cell motility by blocking the integrin-mediated polarity pathway. J Cell Biol 2006;172:619–31.
7. Gozuacik D, Kimchi A. DAPk protein family and cancer. Autophagy 2006;2:74–9.
8. Shields JM, Christy RJ, Yang VW. Identification and characterization of a gene encoding a gut-enriched Kruppel-like factor expressed during growth arrest. J Biol Chem 1996;271:20009–17.
9. Ghaleb AM, McConnell BB, Kaestner KH, Yang VW. Altered intestinal epithelial homeostasis in mice with intestine-specific deletion of the Kruppel-like factor 4 gene. Dev Biol 2011;349:310–20.
10. Choi BJ, Cho YG, Song JW, Kim CJ, Kim SY, Nam SW, et al. Altered expression of the KLF4 in colorectal cancers. Pathol Res Pract 2006;202:585–9.
11. Wei D, Gong W, Kanai M, Schlunk C, Wang L, Yao JC, et al. Drastic down-regulation of Kruppel-like factor 4 expression is critical in human gastric cancer development and progression. Cancer Res 2005; 65:2746–54.
12. Zhao W, Hisamuddin IM, Nandan MO, Babbin BA, Lamb NE, Yang VW, et al. Identification of Kruppel-like factor 4 as a potential tumor suppressor gene in colorectal cancer. Oncogene 2004;23:395–402.
13. Patel NV, Ghaleb AM, Nandan MO, Yang VW. Expression of the tumor suppressor Kruppel-like factor 4 as a prognostic predictor for colon cancer. Cancer Epidemiol Biomarkers Prev 2010;19:2631–8.
14. Ghaleb AM, McConnell BB, Nandan MO, Katz JP, Kaestner KH, Yang VW, et al. Haploinsufficiency of Kruppel-like factor 4 promotes adenomatous polyposis coli dependent intestinal tumorigenesis. Cancer Res 2007;67:7147–54.
15. Dang DT, Chen X, Feng J, Torbenson M, Dang LH, Yang VW, et al. Overexpression of Kruppel-like factor 4 in the human colon cancer cell line RKO leads to reduced tumorigenecity. Oncogene 2003;22: 3424–30.
16. Li R, Liang J, Ni S, Zhou T, Qing X, Li H, et al. A mesenchymal-to-epithelial transition initiates and is required for the nuclear reprogramming of mouse fibroblasts. Cell Stem Cell 2010;7:51–63.
17. Yori JL, Johnson E, Zhou G, Jain MK, Keri RA. Kruppel-like factor 4 inhibits epithelial-to-mesenchymal transition through regulation of E-cadherin gene expression. J Biol Chem 2010;285:16854–63.
18. Wei D, Kanai M, Jia Z, Le X, Xie K. Kruppel-like factor 4 induces p27Kip1 expression in and suppresses the growth and metastasis of human pancreatic cancer cells. Cancer Res 2008;68:4631–9.
19. Bartel DP. MicroRNAs: genomics, biogenesis, mechanism, and function. Cell 2004;116:281–97.
20. He L, Hannon GJ. MicroRNAs: small RNAs with a big role in gene regulation. Nat Rev Genet 2004;5:522–31.
21. Aigner A. MicroRNAs (miRNAs) in cancer invasion and metastasis: therapeutic approaches based on metastasis-related miRNAs. J Mol Med (Berl) 2011;89:445–57.
22. White NM, Fatoohi E, Metias M, Jung K, Stephan C, Yousef GM, et al. Metastamirs: a stepping stone towards improved cancer management. Nat Rev Clin Oncol 2011;8:75–84.
23. Martello G, Rosato A, Ferrari F, Manfrin A, Cordenonsi M, Dupont S, et al. A MicroRNA targeting dicer for metastasis control. Cell 2010; 141:1195–207.
24. Faber C, Horst D, Hlubek F, Kirchner T. Overexpression of Dicer predicts poor survival in colorectal cancer. Eur J Cancer 2011;47: 1414–9.
25. Papachristou DJ, Korpetinou A, Giannopoulou E, Antonacopoulou AG, Papadaki H, Grivas P, et al. Expression of the ribonucleases Drosha, Dicer, and Ago2 in colorectal carcinomas. Virchows Arch 2011; 459:431–40.
26. Bhullar JS, Subhas G, Silberberg B, Tilak J, Andrus L, Decker M, et al. A novel nonoperative orthotopic colorectal cancer murine model using electrocoagulation. J Am Coll Surg 2011;213:54–60; discussion 60–1.
27. Kuo TH, Kubota T, Watanabe M, Furukawa T, Teramoto T, Ishibiki K, et al. Liver colonization competence governs colon cancer metastasis. Proc Natl Acad Sci U S A 1995;92:12085–9.
28. Opolski A, Wietrzyk J, Dus´ D, Kieda C, Matejuk A, Makowska A, et al. Metastatic potential and saccharide antigens expression of human colon cancer cells xenotransplanted into athymic nude mice. Folia Microbiol (Praha) 1998;43:507–10.
29. Rajput A, Dominguez San Martin I, Rose R, Beko A, Levea C, Sharratt E, et al. Characterization of HCT116 human colon cancer cells in an orthotopic model. J Surg Res 2008;147:276–81.
30. Witty JP, McDonnell S, Newell KJ, Cannon P, Navre M, Tressler RJ, et al. Modulation of matrilysin levels in colon carcinoma cell lines affects tumorigenicity *in vivo*. Cancer Res 1994;54:4805–12.
31. John B, Enright AJ, Aravin A, Tuschl T, Sander C, Marks DS, et al. Human MicroRNA targets. PLoS Biol 2004;2:e363.
32. Grimson A, Farh KK, Johnston WK, Garrett-Engele P, Lim LP, Bartel DP, et al. MicroRNA targeting specificity in mammals: determinants beyond seed pairing. Mol Cell 2007;27:91–105.
33. Qiao M, Sheng S, Pardee AB. Metastasis and AKT activation. Cell Cycle 2008;7:2991–6.
34. Finger EC, Giaccia AJ. Hypoxia, inflammation, and the tumor microenvironment in metastatic disease. Cancer Metastasis Rev 2010;29: 285–93.
35. Kulshreshtha R, Ferracin M, Wojcik SE, Garzon R, Alder H, Agosto-Perez FJ, et al. A microRNA signature of hypoxia. Mol Cell Biol 2007; 27:1859–67.
36. Ebert MP, Mooney SH, Tonnes-Priddy L, Lograsso J, Hoffmann J, Chen J, et al. Hypermethylation of the TPEF/HPP1 gene in primary and metastatic colorectal cancers. Neoplasia 2005;7:771–8.
37. Schneider-Stock R, Kuester D, Ullrich O, Mittag F, Habold C, Boltze C, et al. Close localization of DAP-kinase positive tumour-associated macrophages and apoptotic colorectal cancer cells. J Pathol 2006; 209:95–105.
38. Xu XL, Yu J, Zhang HY, Sun MH, Gu J, Du X, et al. Methylation profile of the promoter CpG islands of 31 genes that may contribute to colorectal carcinogenesis. World J Gastroenterol 2004;10:3441–54.
39. Wang WJ, Kuo JC, Ku W, Lee YR, Lin FC, Chang YL, et al. The tumor suppressor DAPK is reciprocally regulated by tyrosine kinase Src and phosphatase LAR. Mol Cell 2007;27:701–16.
40. Tian Y, Luo A, Cai Y, Su Q, Ding F, Chen H, et al. MicroRNA-10b promotes migration and invasion through KLF4 in human esophageal cancer cell lines. J Biol Chem 2010;285:7986–94.
41. Rowland BD, Peeper DS. KLF4, p21 and context-dependent opposing forces in cancer. Nat Rev Cancer 2006;6:11–23.
42. Dong P, Kaneuchi M, Watari H, Hamada J, Sudo S, Ju J, et al. MicroRNA-194 inhibits epithelial to mesenchymal transition of endometrial cancer cells by targeting oncogene BMI-1. Mol Cancer 2011; 10:99.
43. Chen PS, Su JL, Cha ST, Tarn WY, Wang MY, Hsu HC, et al. miR-107 promotes tumor progression by targeting the let-7 microRNA in mice and humans. J Clin Invest 2011;121:3442–55.